EXPERIMENTAL METHODS FOR

IDENTIFYING FAILURE MECHANISMS

I. M. Daniel
Illinois Institute of Technology
Chicago, Illinois

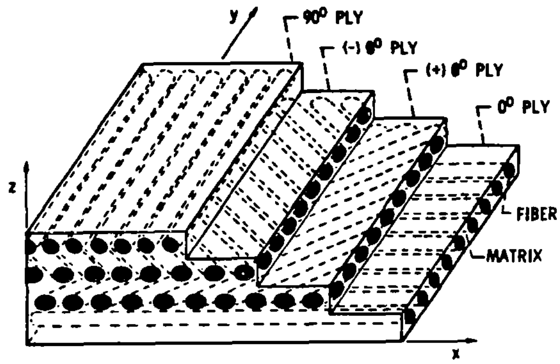

Fiber composite

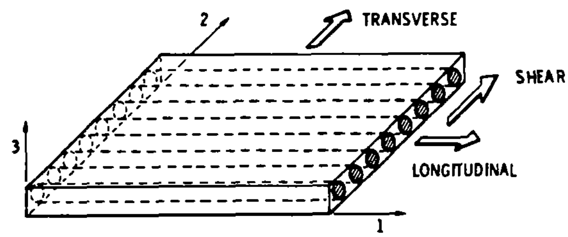

Single ply

<u>MICROSCOPIC</u>

MATRIX FAILURE (TENSILE, COMPRESSIVE, SHEAR)
BOND FAILURE
FIBER FAILURE

<u>MINISCOPIC</u>

FIRST-PLY FAILURE
LAMINA FAILURE CRITERIA

<u>MACROSCOPIC</u>

LAMINATE FAILURE CRITERIA

Scales of observation of failure

1. PHOTOELASTIC (2-D, 3-D, MICROPHOTOELASTIC, DYNAMIC, BIREFRINGENT COMPOSITES, BIREFRINGENT COATINGS)
2. MOIRÉ
3. STRAIN GAGES
4. INTERFEROMETRIC AND HOLOGRAPHIC METHODS
5. NONDESTRUCTIVE EVALUATION (ULTRASONICS, ACOUSTIC EMISSION, X-RAY, THERMOGRAPHY)
6. FRACTOGRAPHY

Experimental methods

STRESS-OPTIC LAW

$$\sigma_1 - \sigma_2 = 2nf/t$$

where

$\sigma_1 - \sigma_2$ = difference of "secondary" principal stresses

n = fringe order

f = material fringe value (constant for material)

t = specimen thickness

Photoelastic method

$$\varepsilon = \frac{1}{S_g} \left(\frac{\Delta R}{R}\right)$$

where

S_g = gage factor (function of alloy and backing of gage)

$$\left(\frac{\Delta R}{R}\right)_{\Delta T} = (\beta-\alpha)\, S_g \Delta T + \gamma \Delta T$$

α = thermal coefficient of expansion of gage material

β = thermal coefficient of expansion of base material

γ = coefficient of resistivity of gage material

Electrical resistance strain gages

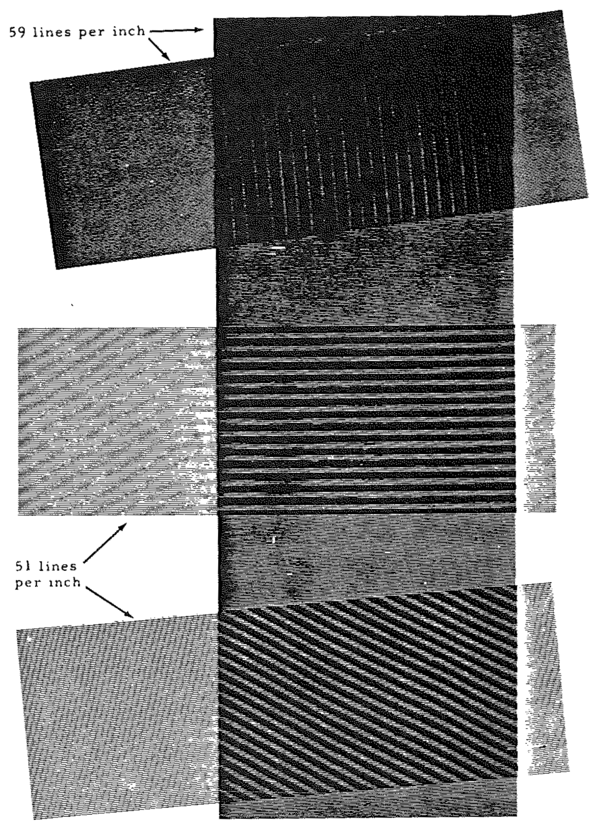

Fringes due to rotation alone

Fringes due to difference in pitch alone

Fringes due to combination of rotation and difference in pitch

Mechanism of formation of Moire fringes

Strain-optic law:

$$\varepsilon_1^c - \varepsilon_2^c = \varepsilon_1^s - \varepsilon_2^s = \frac{Nf_\varepsilon}{2h} = NF_\varepsilon$$

where

f_ε = strain fringe value

N = fringe order

h = coating thickness

c,s = refer to coating and specimen, respectively.

Conditions at boundary:

At interface between coating and specimen,

$$\varepsilon_{22}^c = \varepsilon_{22}^s = -\nu_{12}^s \varepsilon_{11}^s$$

At top surface of coating,

$$\varepsilon_{22}^c = -\nu^c \varepsilon_{11}^c = -\nu^c \varepsilon_{11}^s$$

Principal strain along boundary,

$$\varepsilon_{11}^s = \frac{Nf_\varepsilon}{2h} \cdot \frac{1}{1 + \nu^c}$$

Photoelastic coating method (refs. 1 to 4)

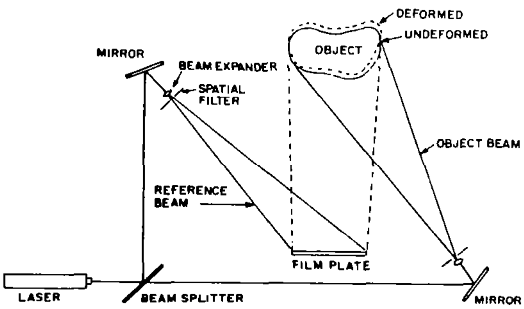

Hologram recording

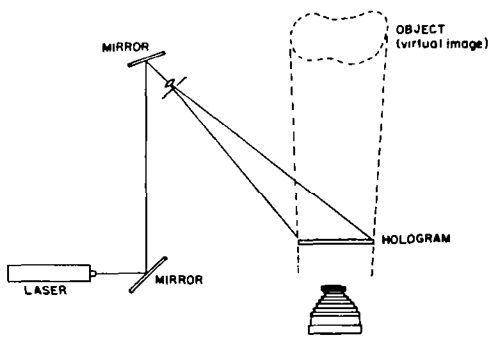

Reconstruction

Holographic processes

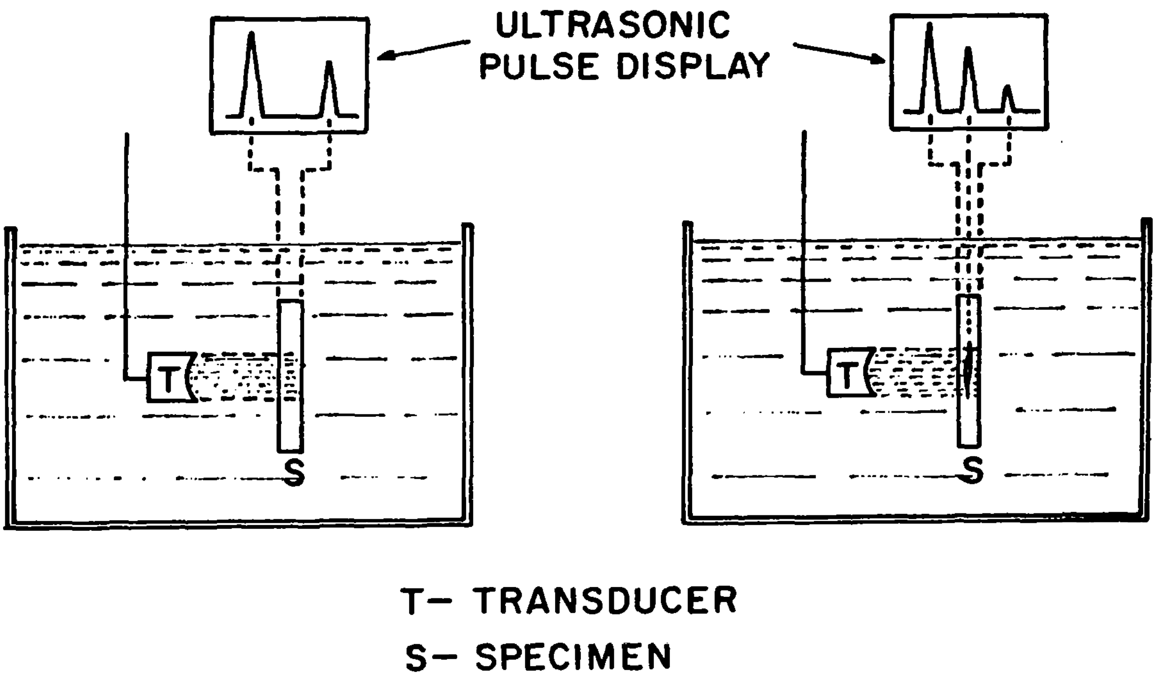

Ultrasonic pulse echo method

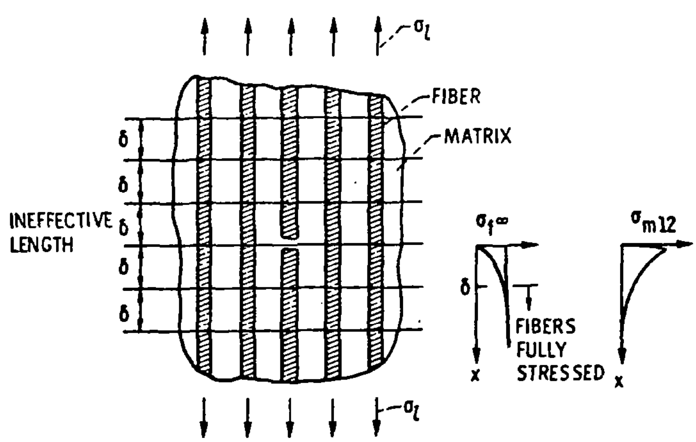

Failure model of unidirectional composite under longitudinal tension (ref. 5)

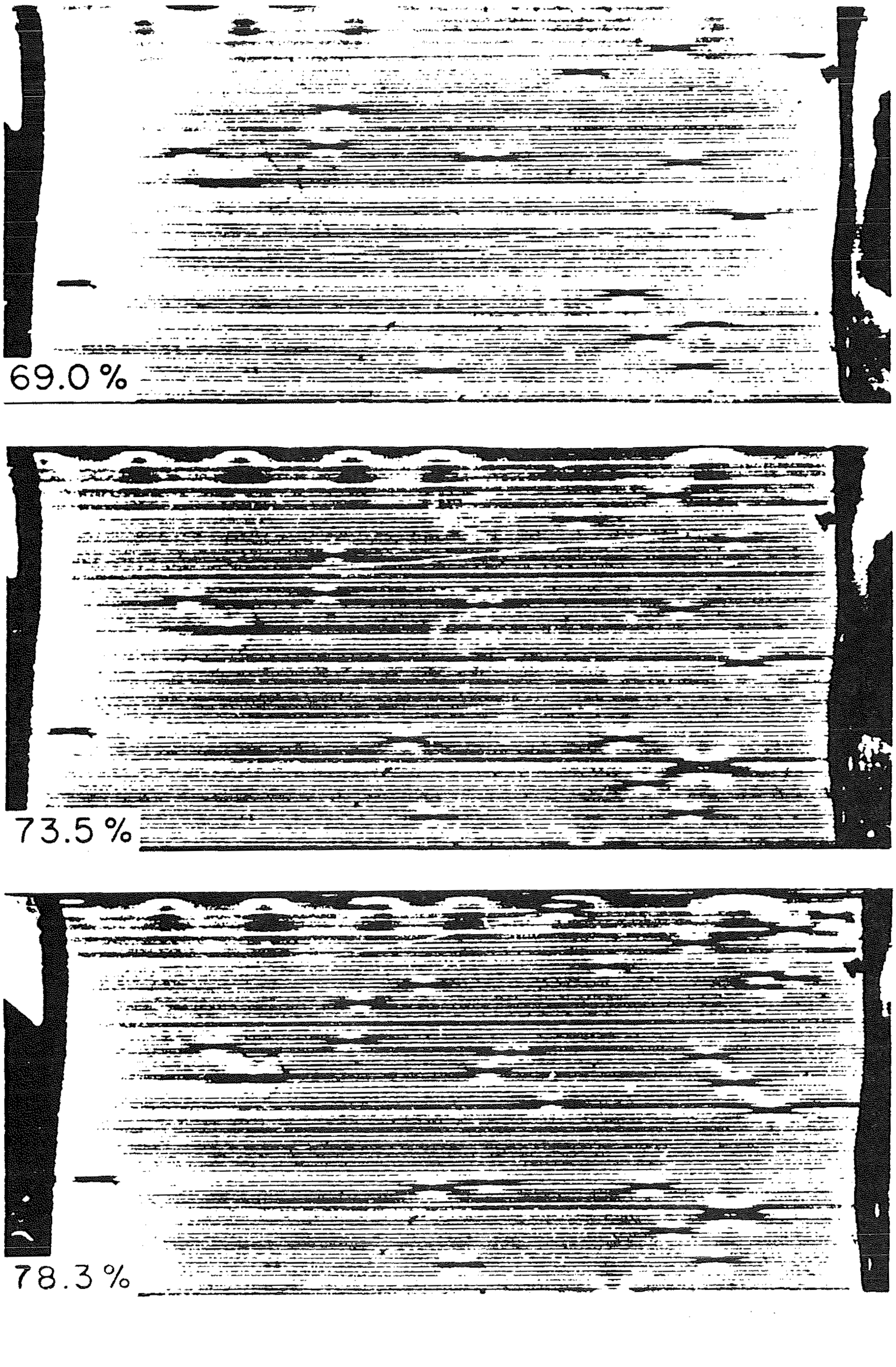

Sequence of photographs showing distribution of fiber breaks
in unidirectional composite under longitudinal tension

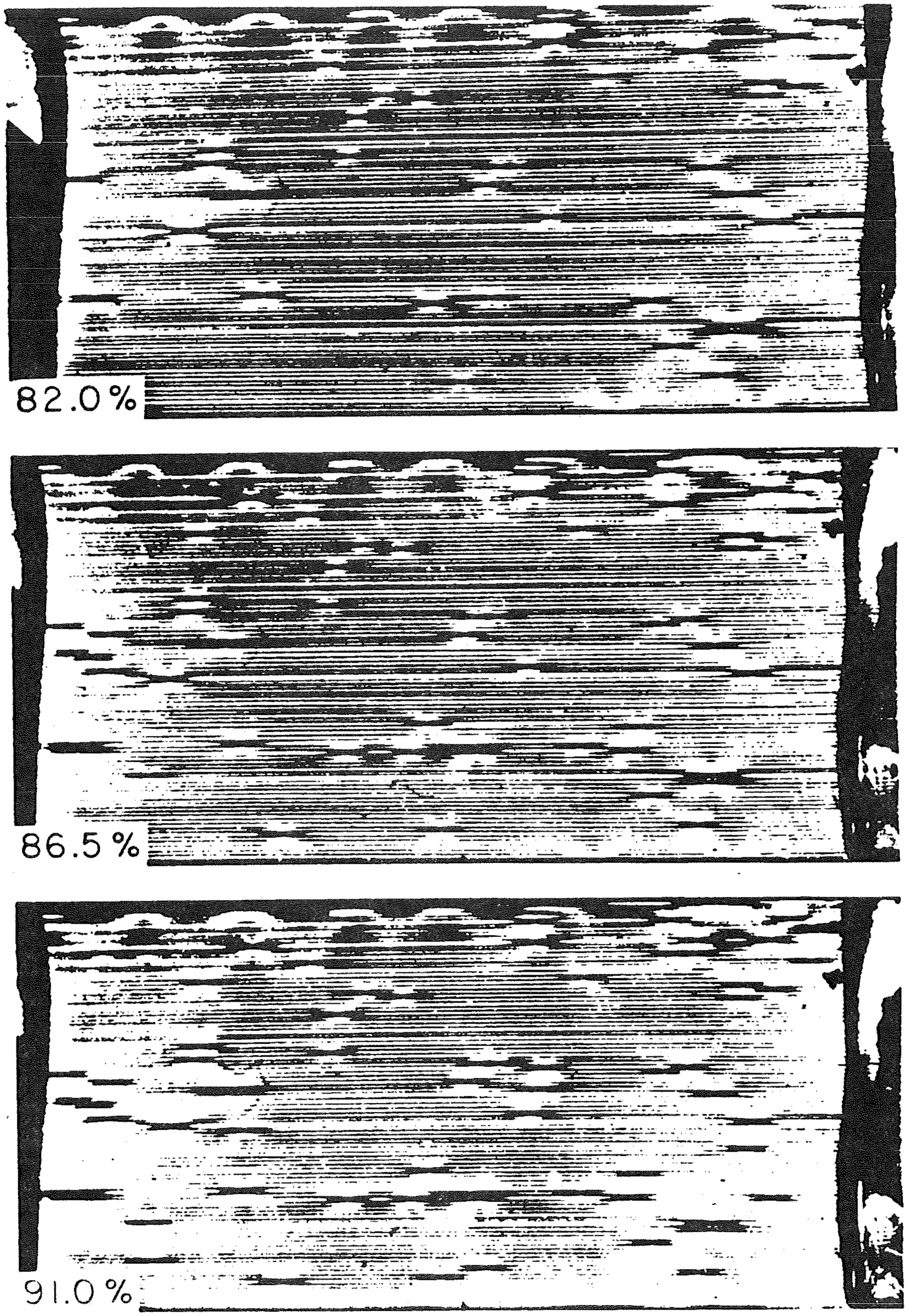

Sequence of photographs showing distribution of fiber breaks in unidirectional composite under longitudinal tension

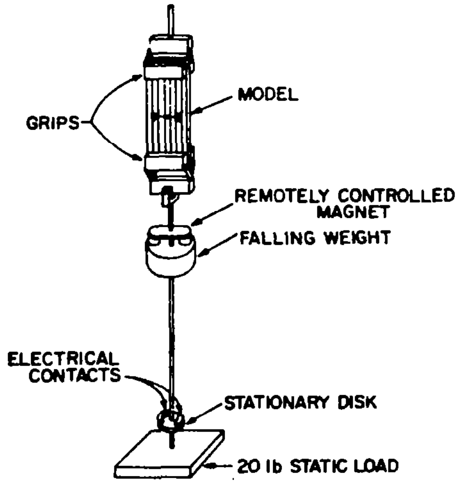

Fixture for dynamic tensile loading of composite models

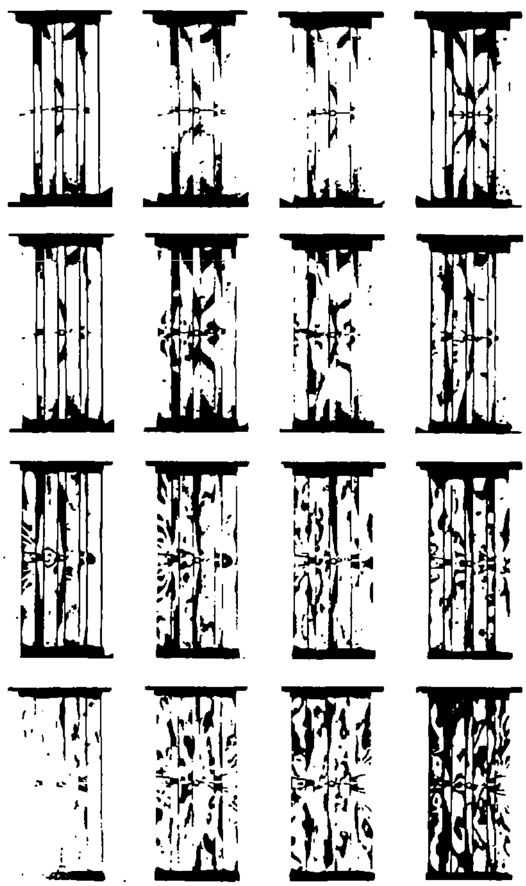

Transient isochromatic fringe patterns in a glass-plastic composite model under dynamic tension (Camera speed: 200,000 frames per second)

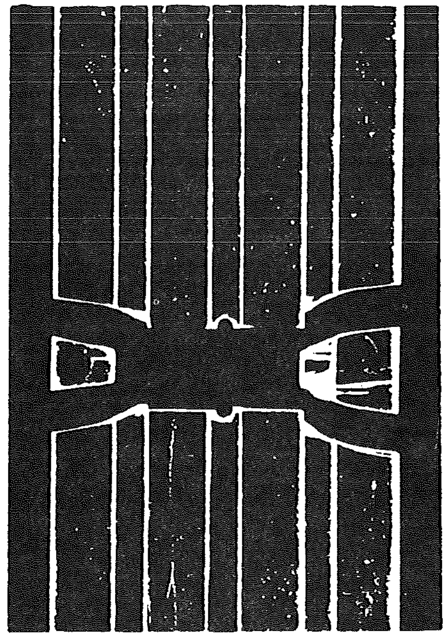

Failure pattern in model of preceding figure

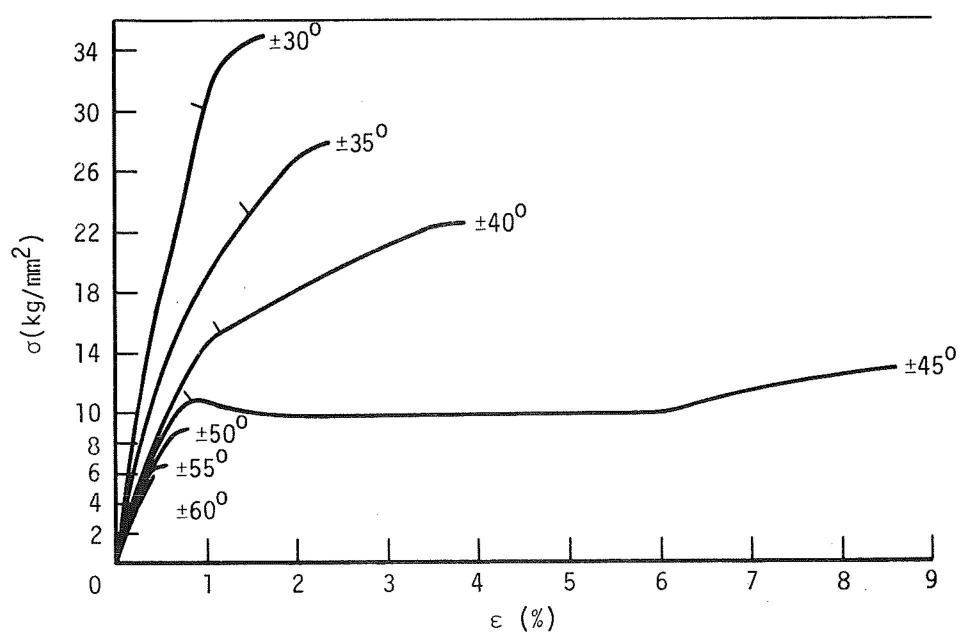

Stress-strain curves of (±θ) angle-ply glass/epoxy laminates

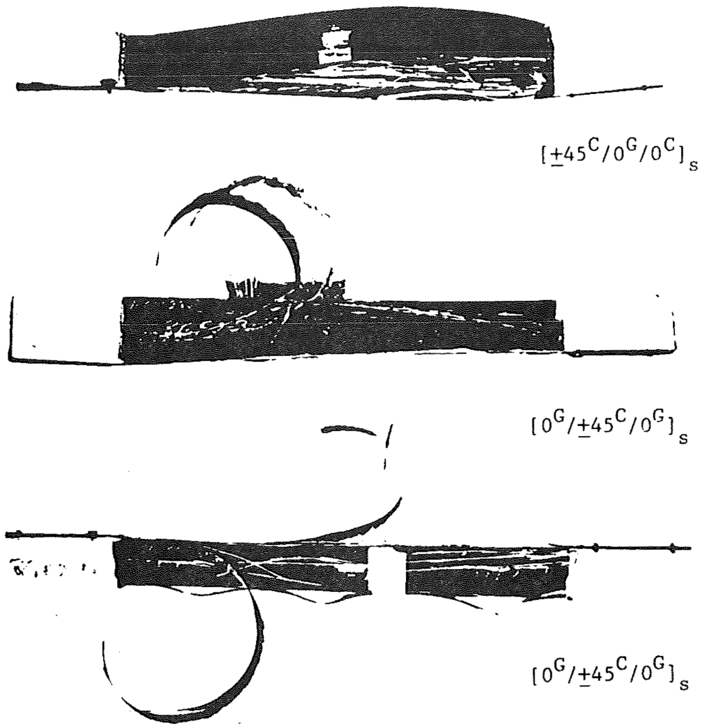

Characteristic failure patterns of three graphite/S-glass/high-modulus epoxy specimens under uniaxial tensile loading

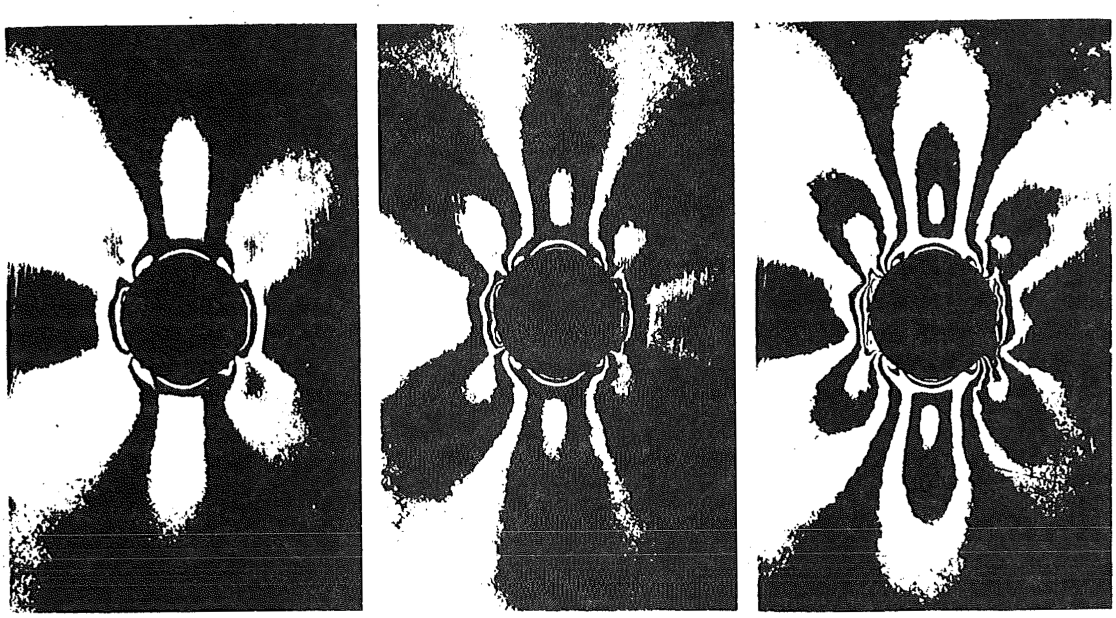

Isochromatic fringe patterns around hole in $[0/\pm45/0/\overline{90}]_s$ boron/epoxy specimen for applied uniaxial stresses of 166 MPa (24.0 ksi), 225 MPa (32.6 ksi), and 293 MPa (42.4 ksi)

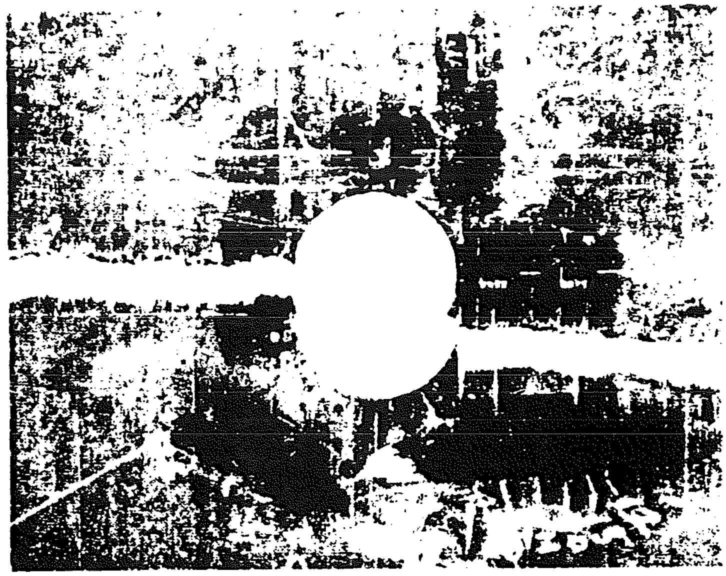

Typical failure pattern around hole in $[0/\pm45/0/\overline{90}]_s$ boron/epoxy specimen under uniaxial tensile loading

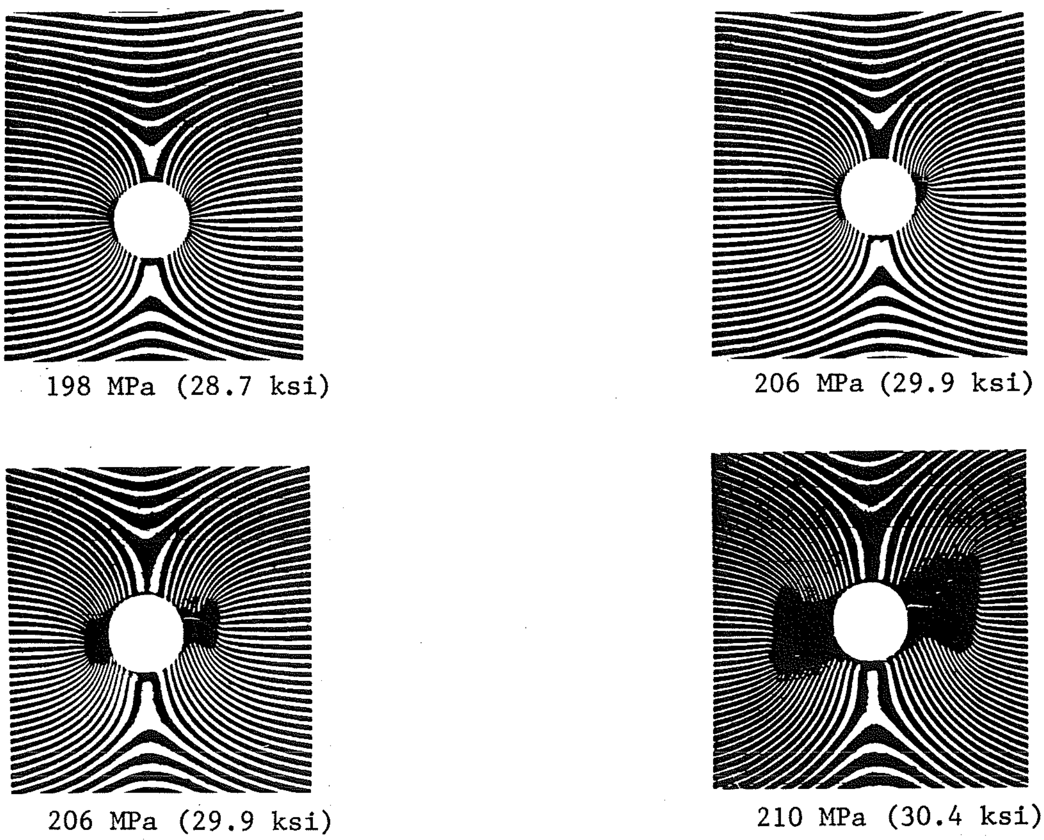

Sequence of Moire fringe patterns corresponding to vertical displacements in $[0/\pm45/0/\overline{90}]_s$ glass/epoxy specimen at various applied uniaxial stresses

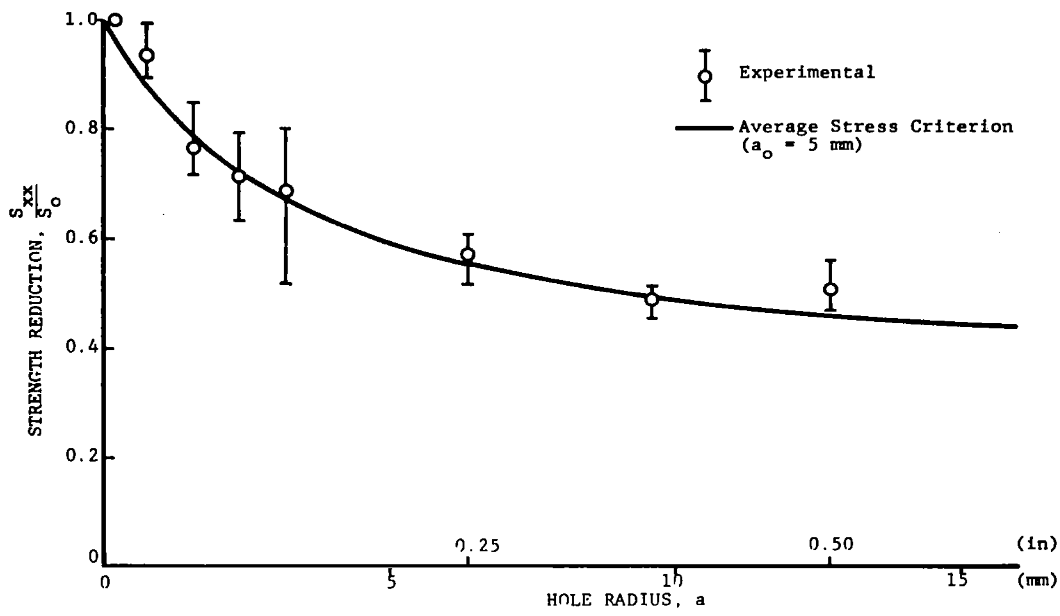

Strength reduction as a function of hole radius for $[0_2/\pm45]_2$ graphite/epoxy plates with circular holes under uniaxial tensile loading

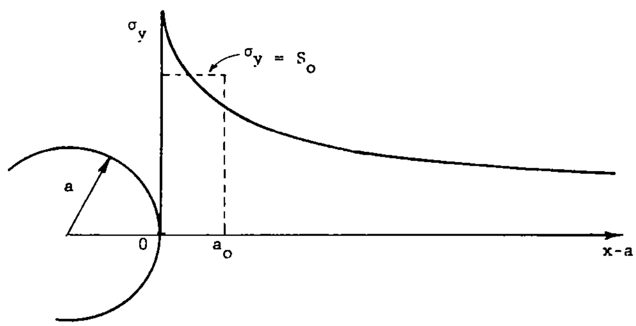

Approximate Stress Distribution

$$\sigma_y \quad (x,0) \quad = \sigma_o \, [1 + \tfrac{1}{2}\rho^{-2} + \tfrac{3}{2}\rho^{-4} + \tfrac{1}{2}(k_\sigma - 3)\,(5\rho^{-6} - 7\rho^{-8})]$$

σ_o = far field stress

ρ = x/a

k_σ = anisotropic stress concentration factor

Strength Reduction Ratio

$$\frac{S_{yy}}{S_o} = \frac{2}{(1+\xi)\;[2 + \xi^2 + (k_\sigma - 3)\,\xi^6]}$$

$$\xi = \frac{a}{a + a_o}$$

a_o = characteristic length dimension

S_{yy}, S_o = strengths of notched and unnotched laminates, respectively.

Strength reduction of uniaxially loaded composite plate with hole according to average stress criterion

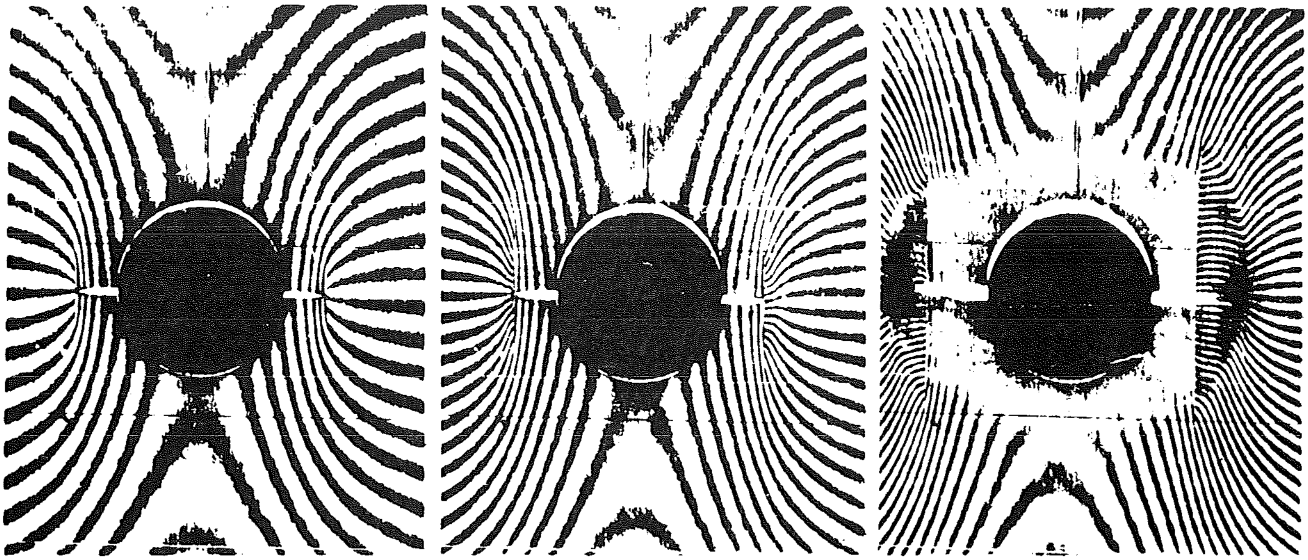

σ_y = 76 MPa (11.0 ksi) σ_y = 102 MPa (14.8 ksi) σ_y = 128 MPa (18.5 ksi)

Moire fringe patterns around crack in glass/epoxy composites $[0/90/0/\overline{90}]_s$ at three levels of applied stress

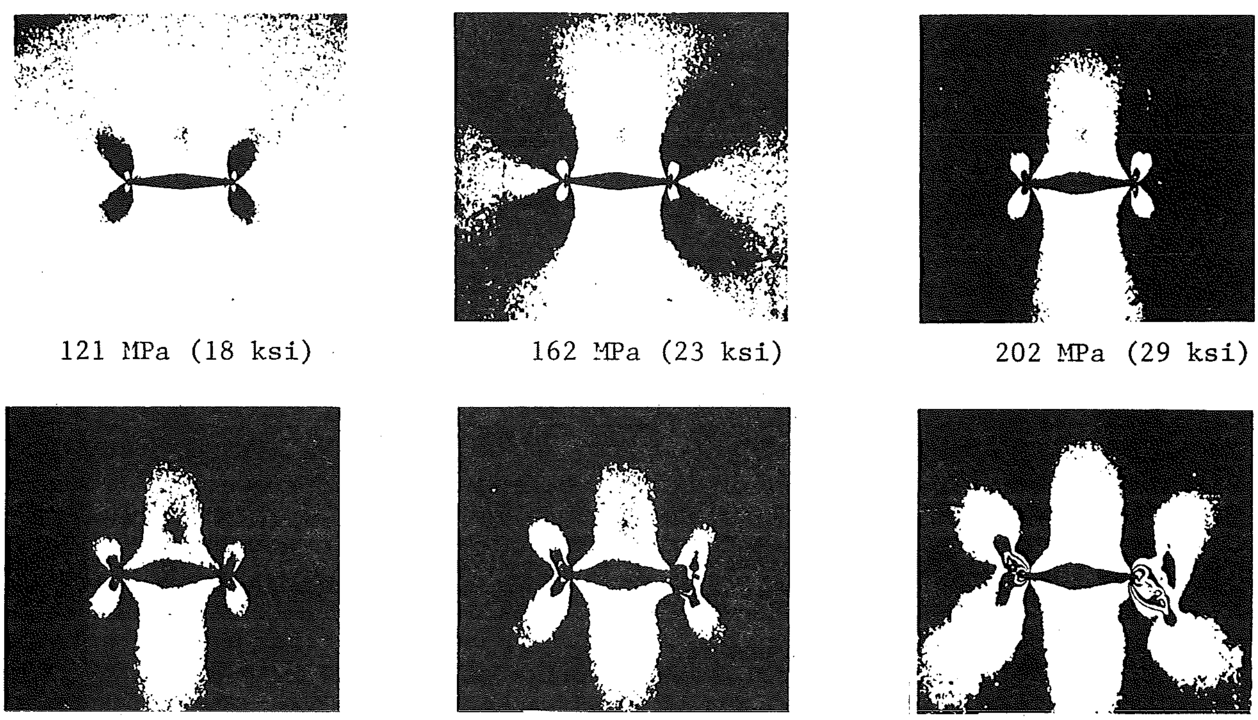

121 MPa (18 ksi) 162 MPa (23 ksi) 202 MPa (29 ksi)

222 MPa (32 ksi) 243 MPa (35 ksi) 273 MPa (40 ksi)

Isochromatic fringe patterns in photoelastic coating around 1.27-cm (0.50 in.) crack of $[0/\pm 45/90]_s$ graphite/epoxy specimen at various levels of applied stress

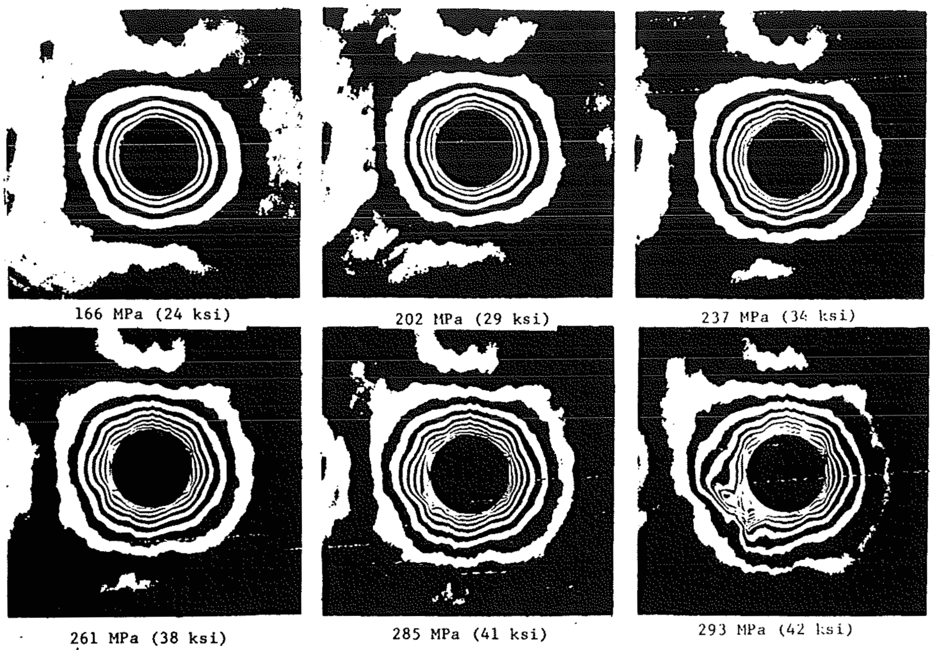

Isochromatic fringe patterns in photoelastic coating of $[0/\pm45/90]_s$ graphite/epoxy specimen with 2.54-cm-diameter (1 in.) hole under equal biaxial tensile loading (Far-field biaxial stress marked)

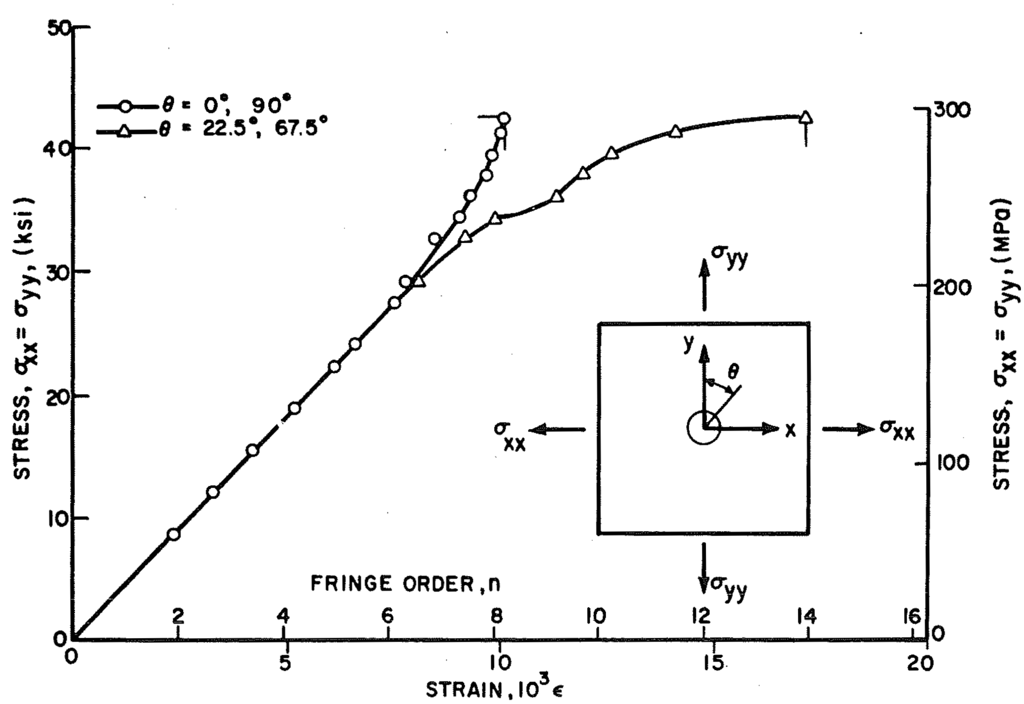

Fringe order and circumferential strain at two locations on the hole boundary for $[0/\pm45/90]_s$ graphite/epoxy specimen with 2.54-cm-diameter (1 in.) hole under equal biaxial loading

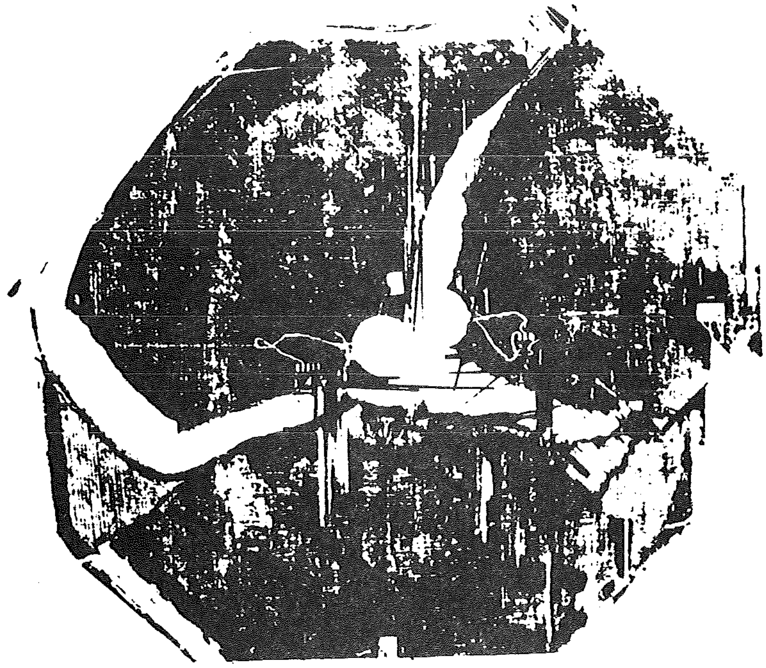

Failure pattern in $[0/\pm 45/90]_S$ graphite/epoxy specimen with 1.91-cm-diameter (0.75 in.) hole under equal biaxial tensile loading

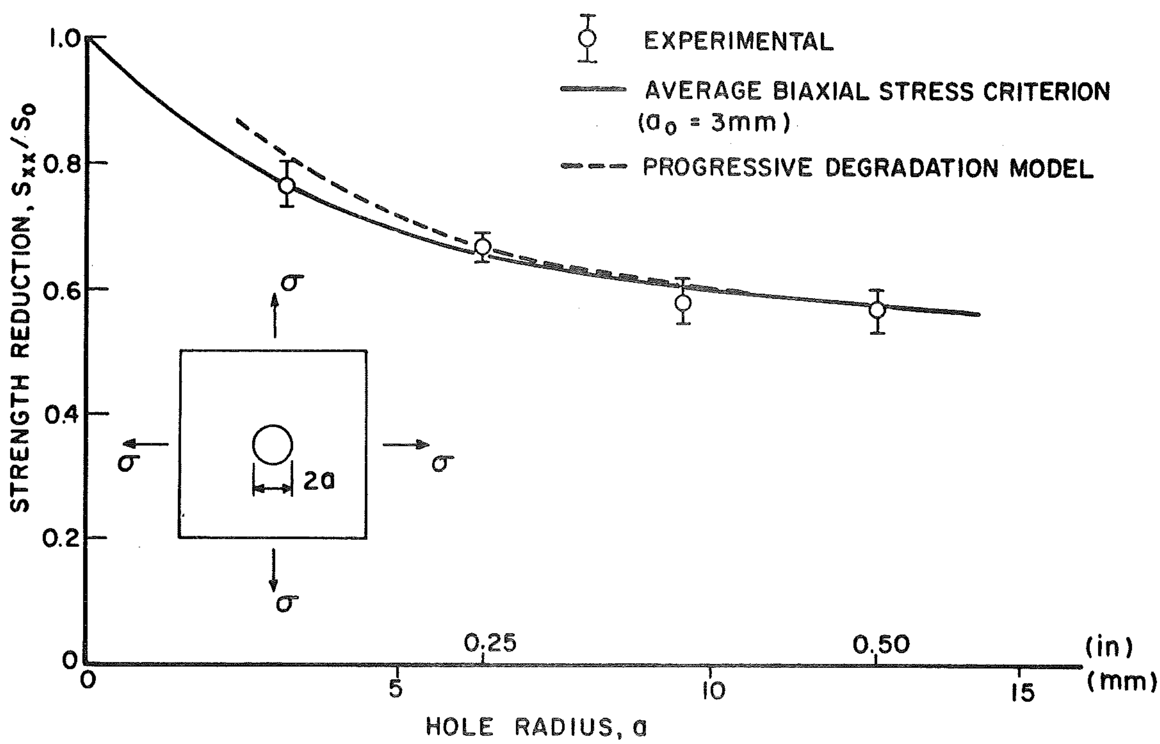

Strength reduction as a function of hole radius for $[0/\pm 45/90]_S$ graphite/epoxy plates with circular holes under 1:1 biaxial tensile loading

σ_{xx} = 152 MPa (22 ksi) σ_{xx} = 202 MPa (29 ksi) σ_{xx} = 253 MPa (37 ksi)

Moire fringe patterns around crack in uniaxially loaded $[0/\pm45/90]_s$ graphite/epoxy specimen for three levels of applied stress

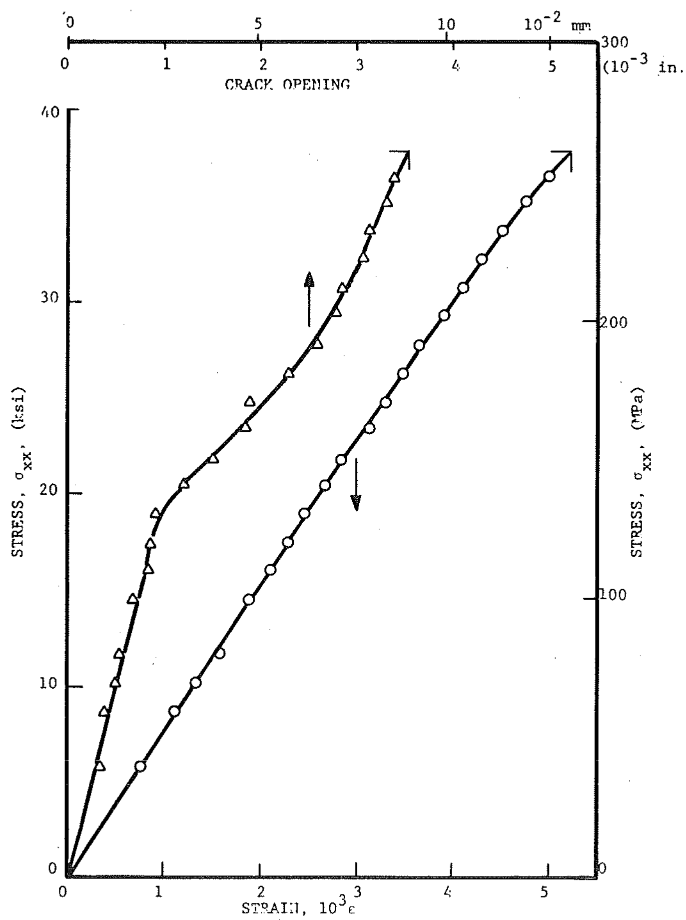

Crack opening displacement and far-field strain for $[0/\pm45/90]_s$ graphite/epoxy specimen with a 1.27-cm (0.50 in.) horizontal crack

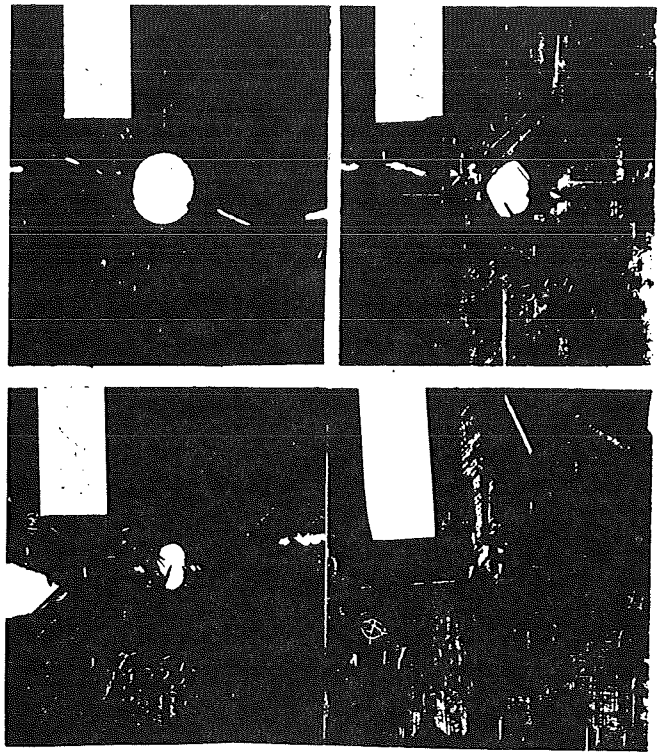

Failure patterns in $[0_2/\pm45]_s$ graphite/epoxy specimens with holes of various sizes under uniaxial tension (Hole diameters are 2.54 cm (1 in.), 1.91 cm (0.75 in.), 1.27 cm (0.50 in.), and 0.64 cm (0.25 in.)

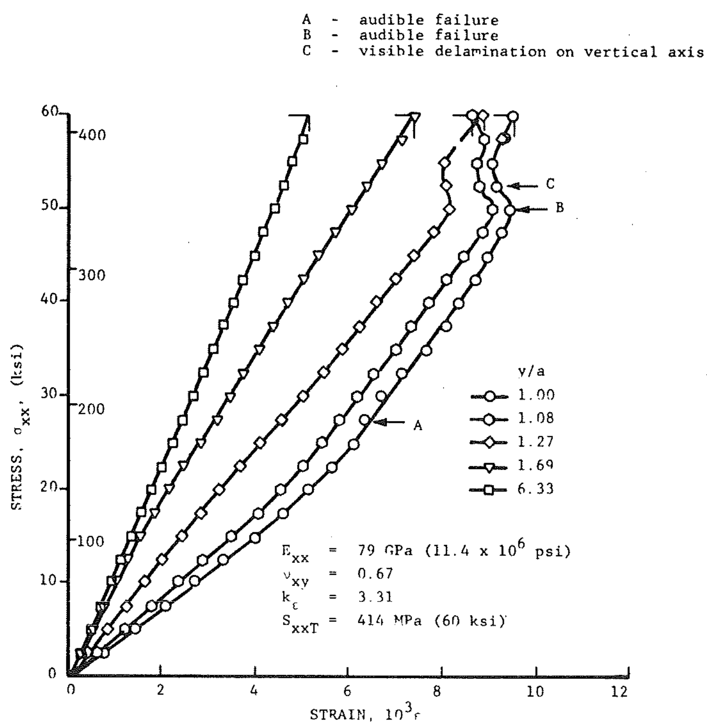

Vertical strains along horizontal axis of $[0_2/\pm45]_s$ graphite/epoxy specimen with 1.91-cm-diameter (0.75 in.) hole under uniaxial tensile loading

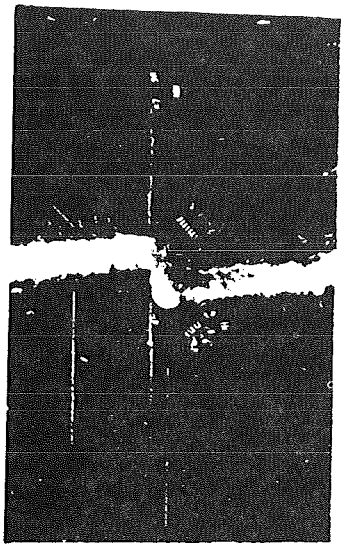

Specimen no. 43; Bo/E; $[\pm 45/0_2/\bar{0}]_s$

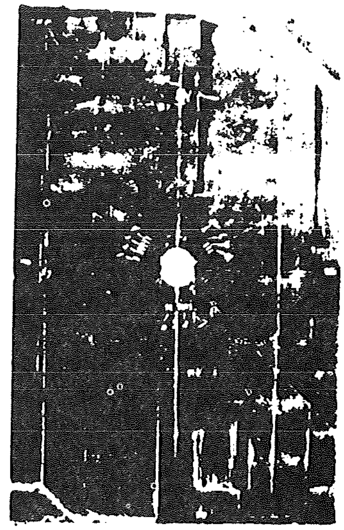

Specimen no. 45; Bo/E; $[0_2/\pm 45/\bar{0}]_s$

Failure patterns of boron-epoxy tensile panels with holes

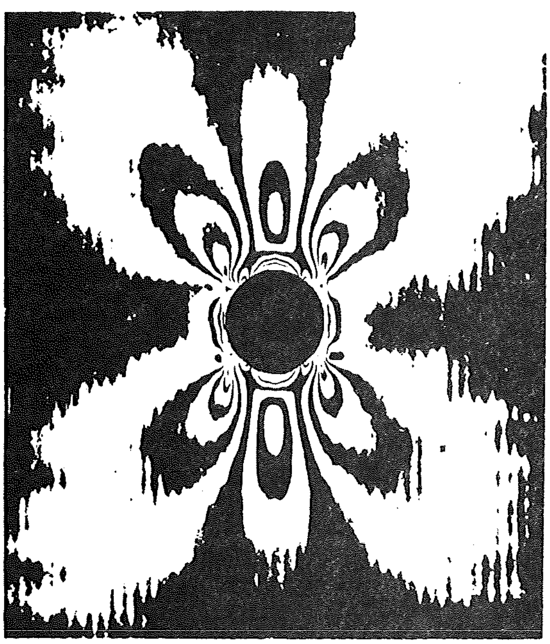

$[0_2/\pm 45/\bar{0}]_s$

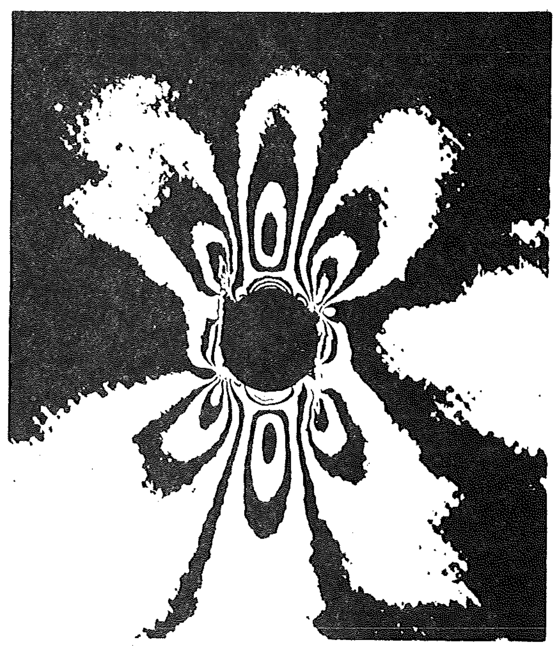

$[\pm 45/0_2/\bar{0}]_s$

Isochromatic fringe patterns in photoelastic coating around hole in boron/epoxy specimens of two different stacking sequences (σ_y = 392 MPa (56.8 ksi))

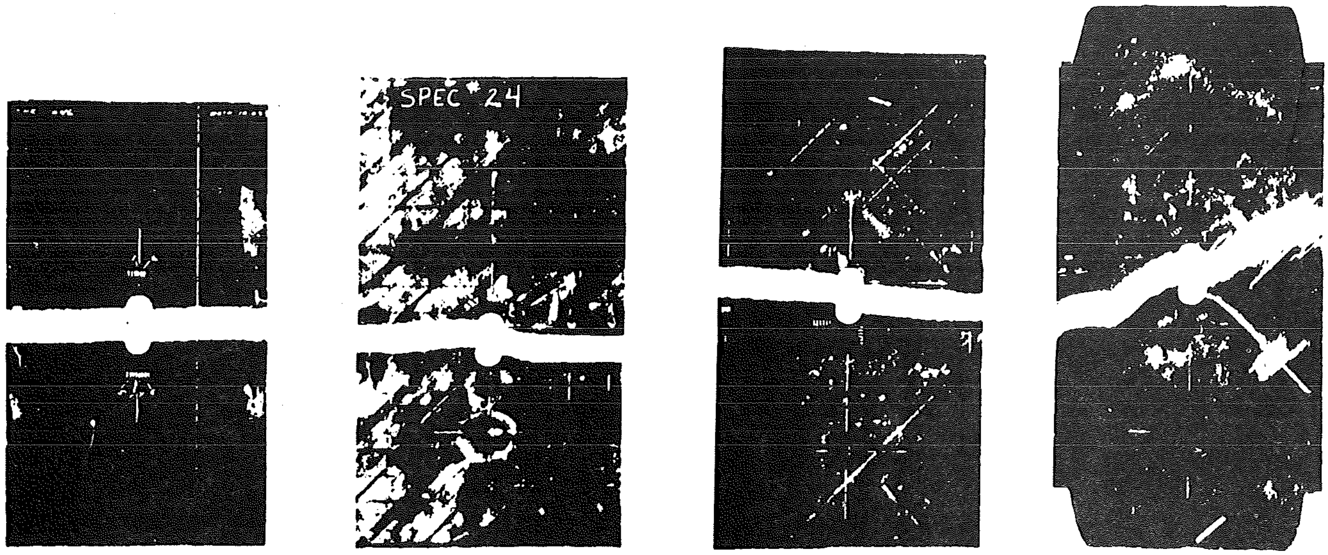

$[0/90/0/90]_s$ $[45/90/0/-45]_s$ $[\pm45/0/\pm45]_s$ $[\pm45/\pm45]_s$

Failure patterns of boron-epoxy panels with holes of various laminate constructions

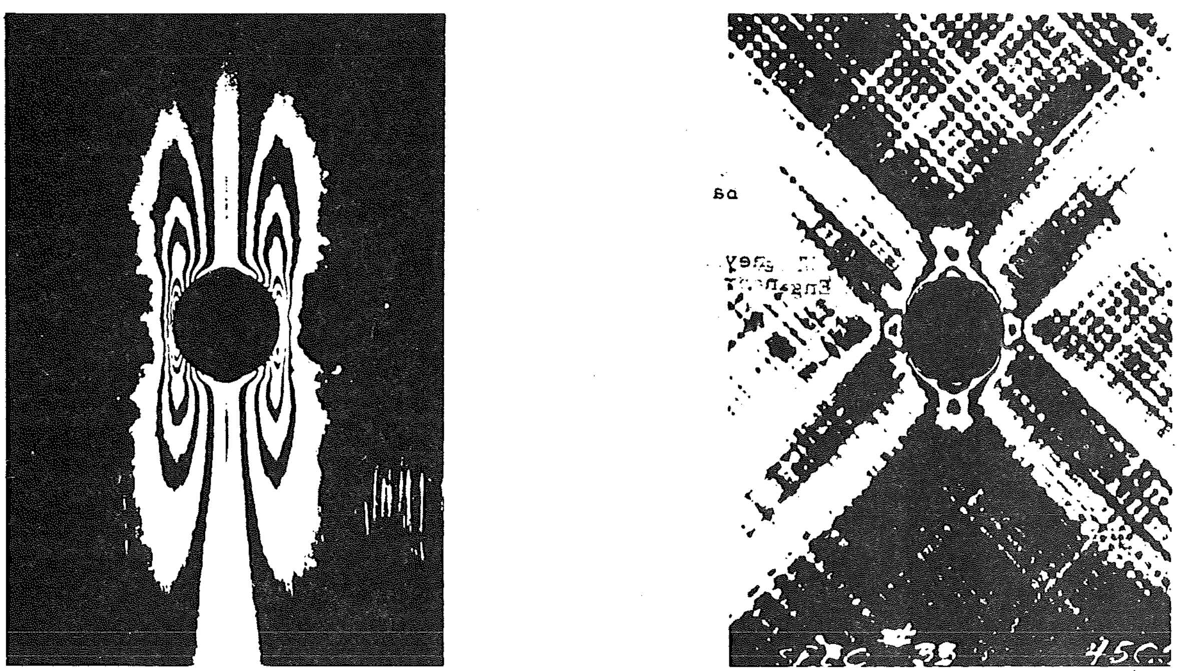

$[0/90/0/90]_s$; σ_y = 170 MPa (24.6 ksi) $[\pm45/\pm45]_s$; σ_y = 77 MPa (11.1 ksi)

Isochromatic fringe patterns in photoelastic coating around hole in boron/epoxy specimens

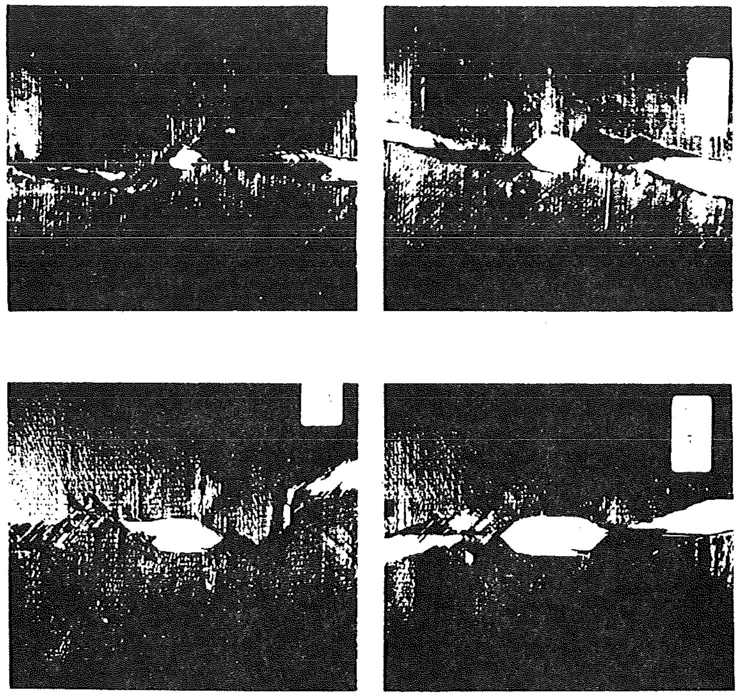

Failure patterns in uniaxially loaded $[0/\pm45/90]_S$ graphite/epoxy plates with cracks of various lengths (Crack lengths are 0.64 cm (0.35 in.), 1.27 cm (0.50 in.), 1.91 cm; (0.75 in.), and 2.54 cm (1.00 in.)

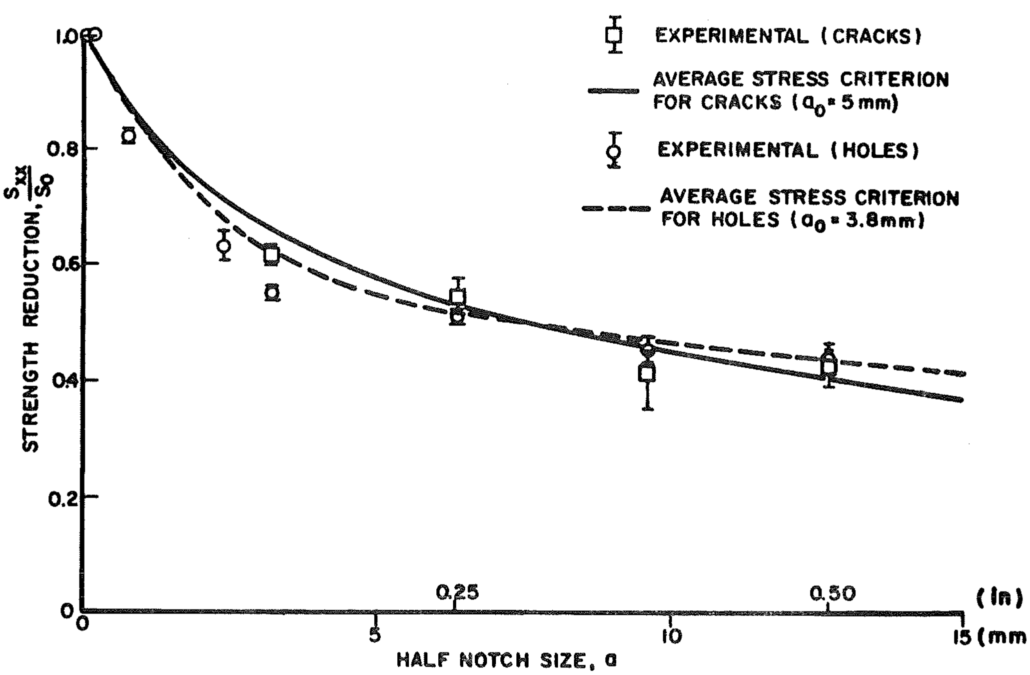

Strength reduction as a function of notch size for $[0/\pm45/90]_S$ graphite/epoxy plates with circular holes and horizontal cracks under uniaxial tensile loading

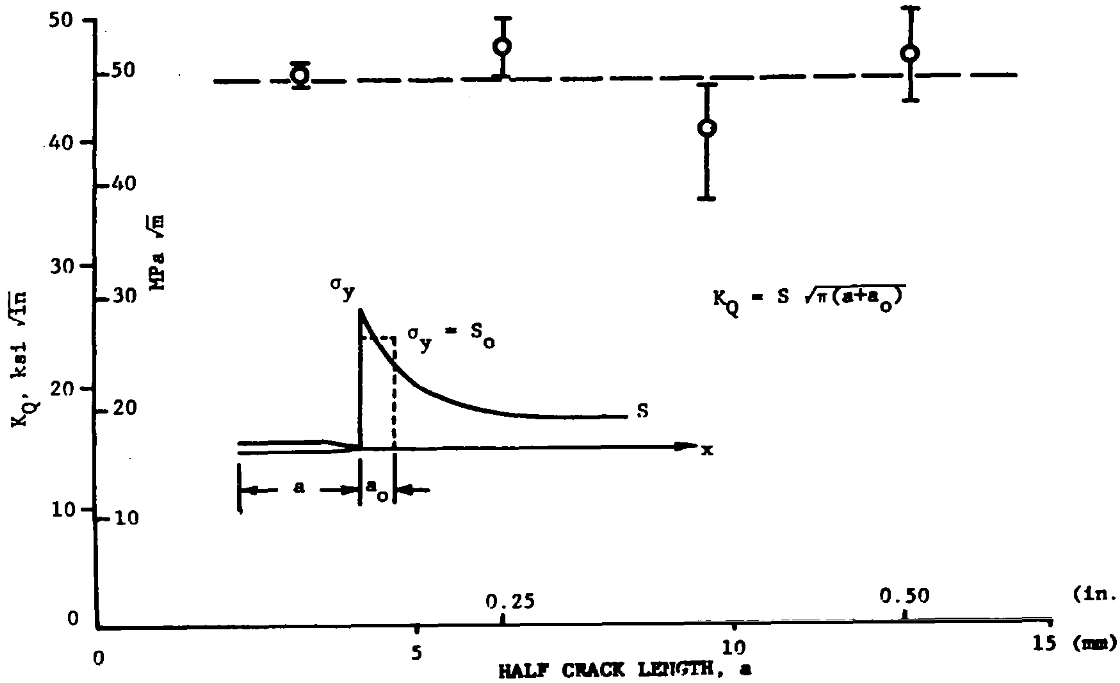

Critical stress intensity factor as a function of crack length for $[0/\pm45/90]_s$ graphite/epoxy plates with horizontal cracks under uniaxial tensile loading

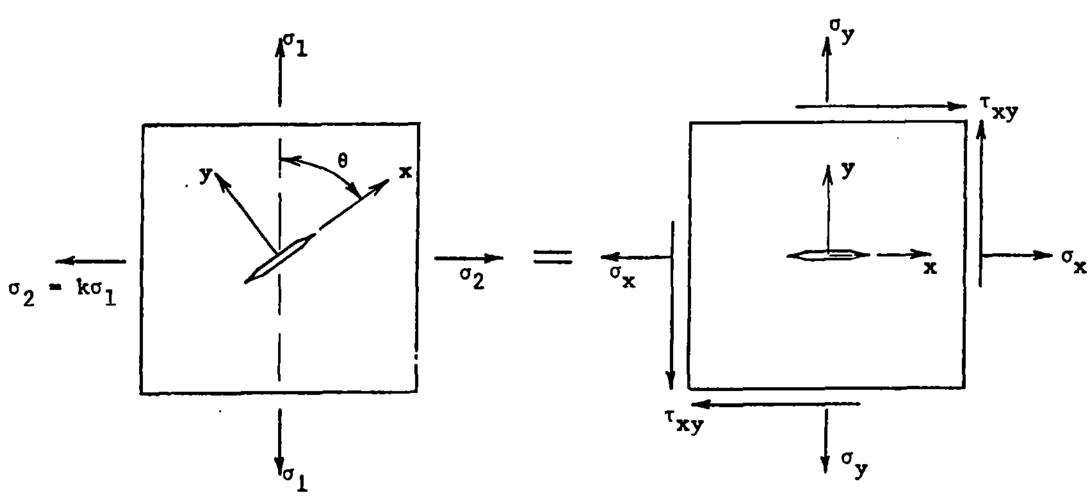

$$\frac{\sigma_y}{\tau_{xy}} = \frac{1 + k - (1-k)\cos 2\theta}{(1-k)\sin 2\theta}$$

Stress transformations of the far-field biaxial state of stress around a crack

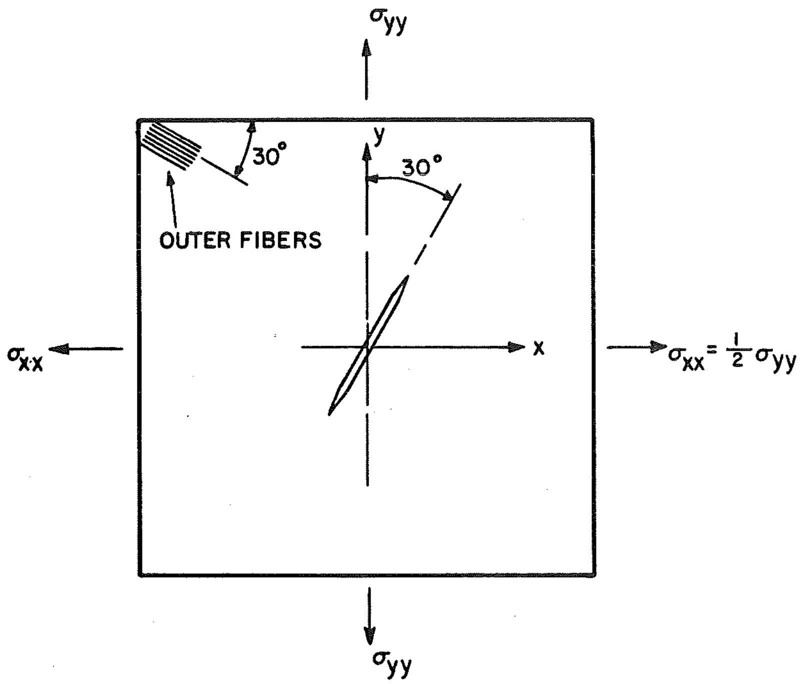

Biaxial loading of $[0/\pm45/90]_s$ graphite/epoxy specimens with cracks

σ_{yy} = 392 MPa (42.4 ksi)

σ_{yy} = 303 MPa (43.9 ksi)

σ_{yy} = 260 MPa (37.7 ksi)

σ_{yy} = 278 MPa (40.3 ksi)

Isochromatic fringe patterns in photoelastic coating around 1.27-cm (0.5 in.) crack in $(0/\pm45/90)_s$ graphite/epoxy specimen under biaxial loading - $\sigma_{yy} = 2.03\sigma_{xx}$ at 30 deg with crack direction

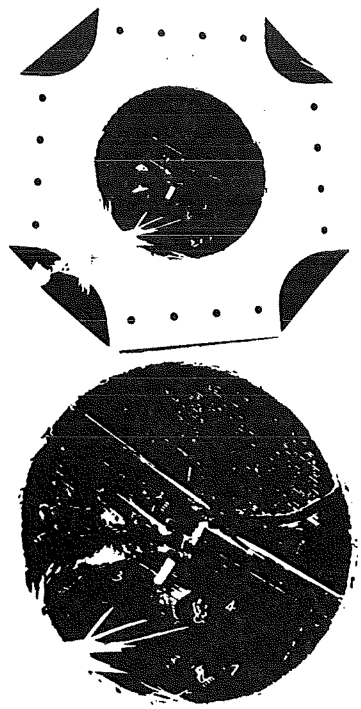

Biaxial specimen with 1.91-cm-long (0.75 in.) crack after failure

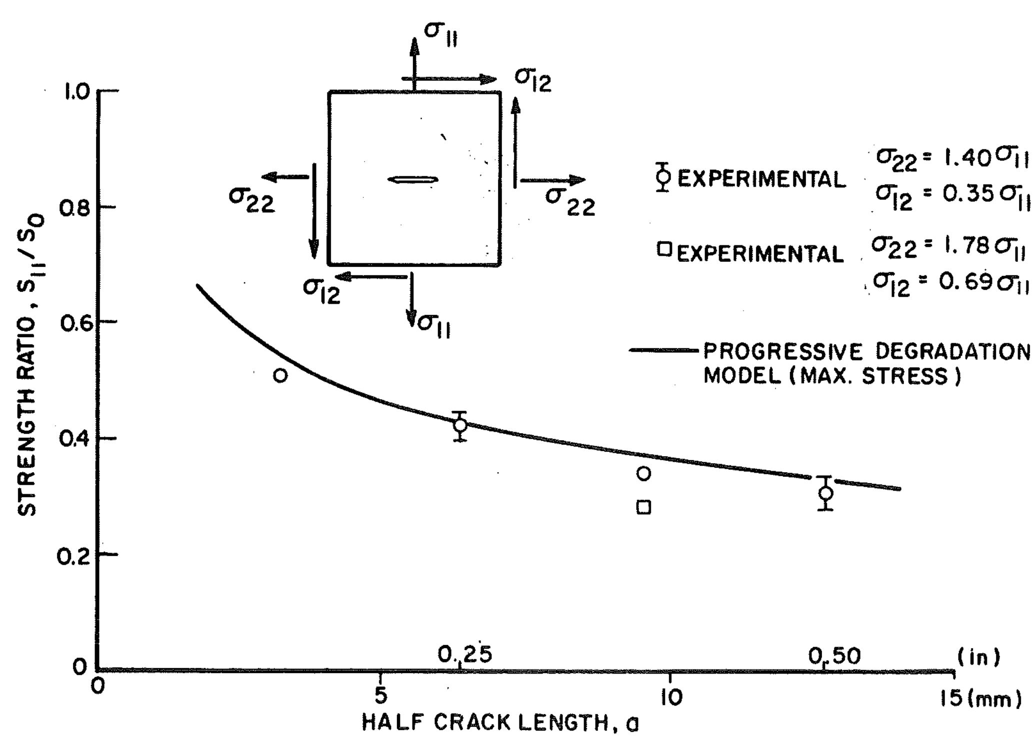

Comparison of experimental and theoretical results for strength ratio for $[0/\pm45/90]_s$ graphite/epoxy plates with cracks under biaxial loading

Front surface

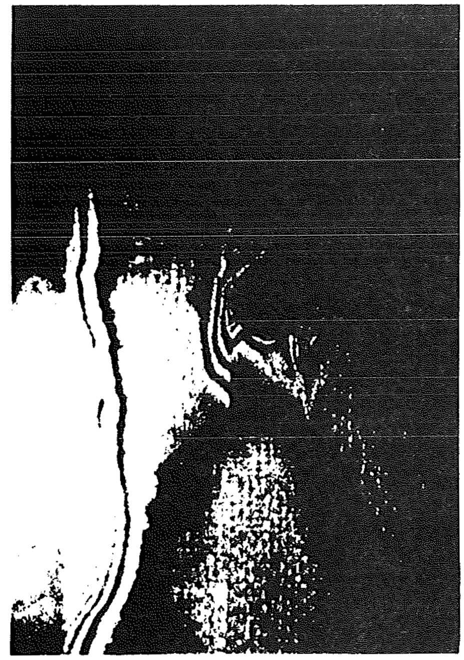

Back surface as viewed from the front through the specimen (ref. 6)

Thermally induced holographic fringe patterns in fatigue-loaded $[0/\pm 45/90]_s$ graphite/epoxy specimen with circular hole

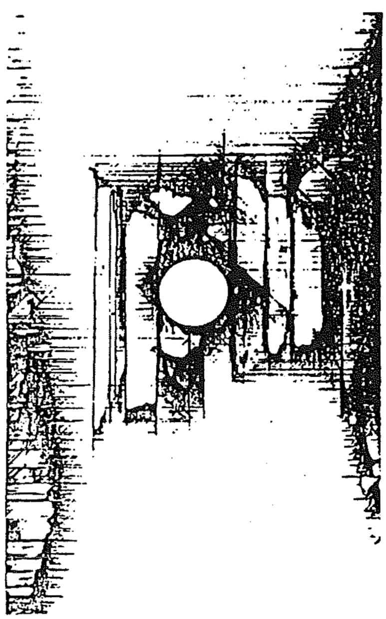

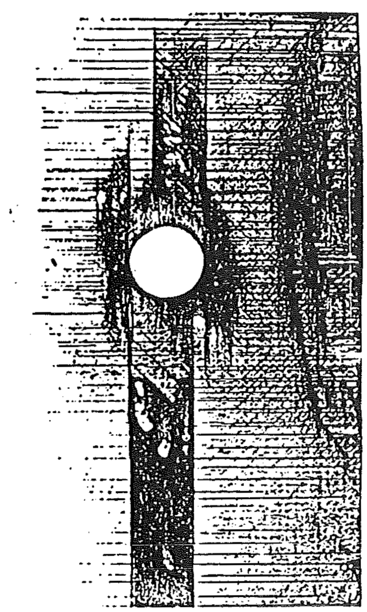

TBE enhanced X-ray photographs showing fatigue-induced damage in $[(0/\pm 45/90)_s]_2$ graphite/epoxy specimens

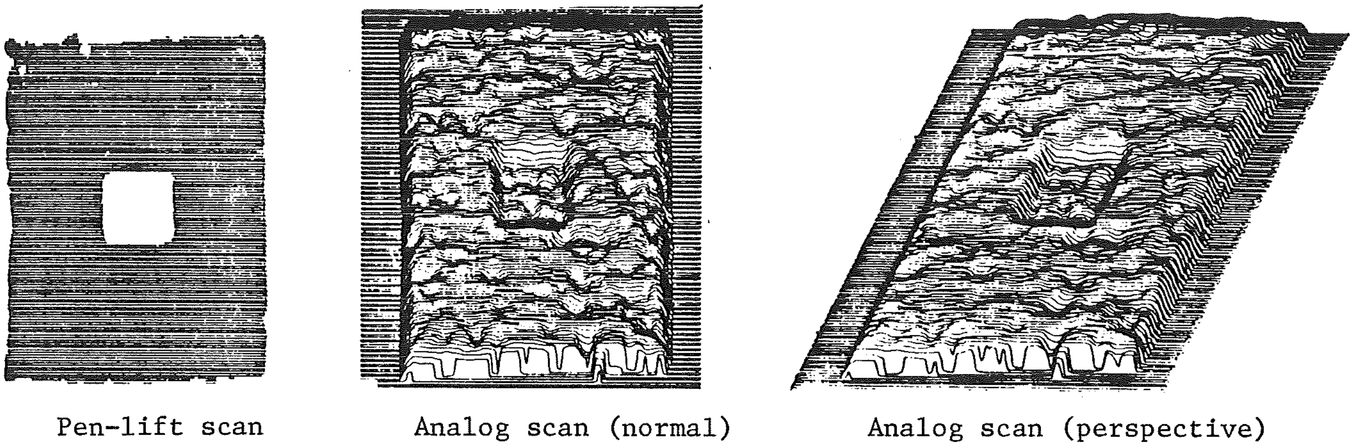

Ultrasonic C-scans of $[0/\pm45/90)_s]_2$ graphite/epoxy specimen with a film patch

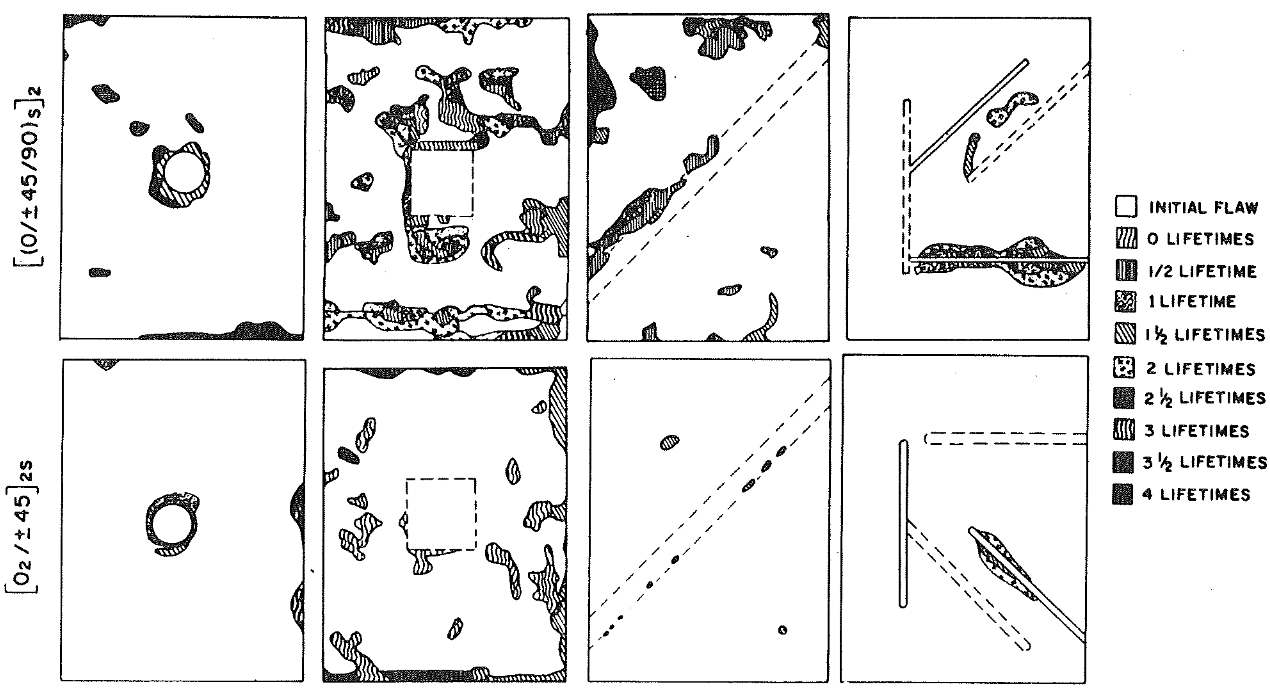

Flaw growth under spectrum fatigue loading in $[(0/\pm45/90)_s]_2$ and $[0_2/\pm45]_{2s}$ graphite/epoxy specimens with four types of initial flaws (Ambient environment)

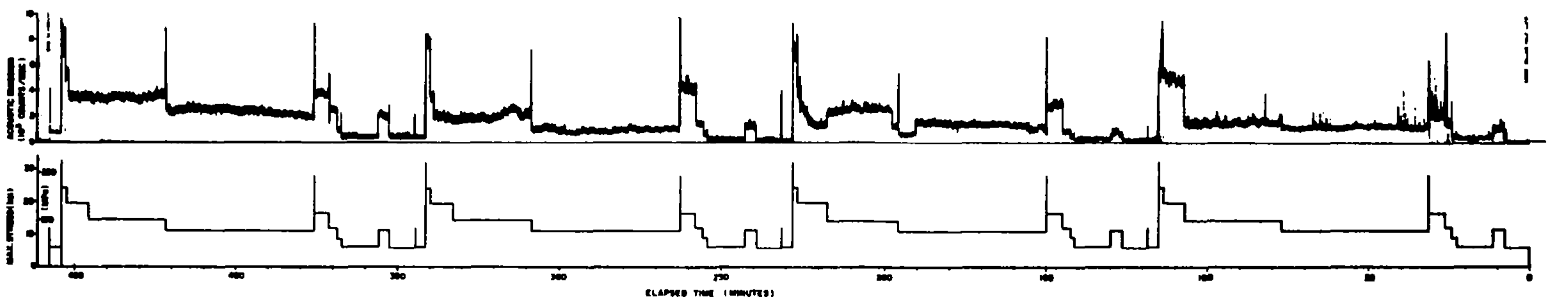

Acoustic emission and corresponding load spectrum as a function of elapsed time for $[0_2/\pm 45]_{2s}$ graphite/epoxy specimens with holes (Time increases from right to left)

REFERENCES

1. Daniel, I. M.; and Rowlands, R. E.: Experimental Stress Analysis of Composite Materials. ASME paper no. 72-DE-6, 1972.

2. Daniel, I. M.: Optical Methods for Testing Composite Materials - Stress Analysis and Fracture Mechanics. Failure Models of Composite Materials With Organic Matrices and Their Consequences on Design, AGARD Conference Proceedings no. 163, 1975.

3. Whitney, J. M.; Daniel, I. M.; and Pipes, R. B.: Experimental Mechanics of Fiber-Reinforces Composite Materials. SESA monograph no. 4, Society for Experimental Stress Analysis, 1982.

4. Dally, J. W.; and Alfirevicn, I.: Application of Birefringent Coatings to Glass-Fiber-Reinforced Plastics. Exper. Mech., vol. 9, 1969, pp. 97-102.

5. Rosen, B. Walter: Mechanics of Composite Strengthening. Fiber Composite Materials, American Society for Metals, 1965, pp. 37-75.

6. Krautkraemer, J.; and Krautkraemer, H.: Ultrasonic Testing of Materials. Springer-Verlag, New York, 1977.